JOURNAL OF MATERIALS SCIENCE **35** (2000) 3121–3126

Short range ordering in amorphous In-Se films by wide-angle X-ray scattering

A. BURIAN
Institute of Physics, University of Silesia, ul. Uniwersytecka 4, 40-007 Katowice, Poland and Centre of Polymer Chemistry, Polish Academy of Sciences, ul. M. Skłodowskiej-Curie 34, 41-819 Zabrze, Poland
E-mail: burian@us.edu.pl

A. M. BURIAN, J. WESZKA
Centre of Polymer Chemistry, Polish Academy of Sciences, ul. M. Skłodowskiej-Curie 34, 41-819 Zabrze, Poland

M. ŻELECHOWER
Department of Materials Science, Silesian University of Technology, ul. Krasińskiego 8, 40-019 Katowice, Poland

P. LECANTE
CEMES/CNRS, 29, rue J. Marvig, BP 4347, 31055 Toulouse Cedex, France

Wide-angle X-ray scattering studies were performed on In-Se amorphous films, obtained by thermal evaporation, with selenium content of 60 and 66 at.%. The intensities were recorded in the scattering vector range between 3 and 160 nm^{-1}. Structural information about the local structure of the amorphous In-Se films has been derived from the radial distribution function using the curve-fitting method. The experimental results have been compared with model based simulations. The obtained structural parameters indicate that for $In_{40}Se_{60}$ In-In, In-Se and Se-Se contributions are involved in the near-neighbour coordination sphere. As the Se content is increased, the number of In-In bonds is reduced to zero, within the precision of the method. For both amorphous films In is tetrahedrally coordinated while Se has three near neighbours on the average.

1. Introduction

In recent years, compounds of indium and selenium have attracted attention because of their potential applications. In_2Se_3 and InSe have layered structures and may exist as many phases [1–4]. The most important characteristic of these compounds is that they form strong covalent bonds within layer and have weak interlayer interaction of the Van der Waals type. In thin film form, both crystalline and amorphous, indium selenide compounds have suitable electrical and optical properties for applications as solar cells [5, 6] and as switching elements for memory applications [7]. The layered structure of the In-Se films make them attractive material for intercalation and a potential application in lithium batteries [8].

Although the In-Se films have been investigated mainly in crystalline form, the electrical and optical properties of amorphous films have been recently studied [7, 9–12]. In-Se with a Se content of about 75 at.% can be obtained as glass with n-type conduction when doped with Pb [13]. However, the local structure of amorphous In-Se has not been investigated in detail. The hypothesis about a preservation of the local structure of the corresponding crystal in amorphous semiconductors suggests other possibility of application of the amorphous In-Se films. Owing to the layered structure, which is typical for these materials, a low density of dangling bonds is expected [14]. This property makes it possible to produce heterojunction devices with a low interface density of states.

The main aim of this work is to study local or short-range ordering in the amorphous In-Se films obtained by thermal evaporation. Such a characterization of amorphous materials is essential for understanding their electrical and optical properties.

2. Experimental techniques

The starting materials were prepared by mixing quantities of high purity (5N) of indium and selenium pellets in the 2 : 3 and 1 : 2 proportions. The mixtures were sealed in evacuated quartz ampoules and heated at about 1250 K for 24 h and then slowly cooled down to room temperature. The amorphous films were obtained by thermal evaporation of the bulk polycrystalline In-Se materials onto glass substrates maintained at room

temperature. The substrates were cleaned ultrasonically in absolute ethanol. The deposition was performed at a pressure of 10^{-3} Pa. The source material was evaporated from a molybdenum boat which had a multihole cover to avoid escaping of the powdered material from the boat during evaporation. This method was applied to obtain the In-Se films with controlled composition [11, 12]. The glass substrates were placed about 15 cm above the boat. A high deposition rate (not less than 15 nm/s) was employed to reduce effect of the dissipation of volatile selenium during evaporation, which may preclude formation of the films with controllable composition at a low deposition rate [15]. These difficulties arise from the mechanism of the evaporation of In-Se, which vaporize mainly as In_2Se and Se_2 or other Se cluster [10, 16]. The final film thicknesses of 40–50 μm were achieved after series (usually about 10) of 5-min evaporation runs.

Quantitative analysis of the chemical composition of the amorphous films was performed by electron microprobe analysis. The investigated films, containing In and Se, have been examined using a JSM35 scanning electron microscope attached with a LINK290 energy dispersive X-ray spectrometer. High voltage of 25 kV and a probe current of $2 \cdot 10^{-10}$ A were applied. The Monte Carlo simulation software [17] was used before measurements in order to estimate an electrons penetration depth and then to choose an appropriate high voltage. Kα X-ray line of selenium and Lα line of indium were selected for quantification. Several measurements of the intensities of the X-ray lines in different points on the specimen surface were performed in order to get satisfactory statistics and then the corresponding standard deviations were computed. In_2Se_3 single crystal has been used as a standard and the ZAF correction routine [18], modified by the convergence to k-ratios [19], was applied to obtain true elemental compositions.

The X-ray scattering data were collected using a diffractometer attached with a molybdenum target tube, a flat graphite monochromator mounted in the incident beam and an evacuated chamber between a sample holder and a scintillation detector. The measurements were carried out in a symmetrical reflection geometry. The data were recorded in the scattering vector range between 3 and 160 nm^{-1} (the scattering vector is $K = 4\pi \sin\theta/\lambda$, where 2θ is the scattering angle and λ is the wavelength). A main disadvantage of the diffractometer with the incident beam monochromator is that fluorescence radiation, possibly excited in a sample, is recorded by the detector. This extra radiation, which cannot be eliminated by the scintillation detector, may lead to serious problems with normalization of the data. However, when the product μt (μ is the linear absorption coefficient and t is the thickness of the specimen, expressed in cm^{-1} and cm, respectively) is of about 2 (here 1.5–1.75) the fluorescence contribution is practically angle independent [20] and can be easily subtracted [21, 22]. The correction method developed for a symmetrical transmission geometry was adapted for the case of the reflection geometry according to [22]. The data were then normalized to electron units using the correction procedures described in detail in our previous paper [22].

TABLE I Compositions of the In-Se films obtained by thermal evaporation

Atomic ratio of the starting material	Composition of the amorphous films (at.% ±1.5)
In : Se	In : Se
2 : 3	40 : 60
1 : 2	34 : 66

3. Results

The compositions of the evaporated films, measured by microprobe analysis, are presented in Table I. These results show that the compositions of the films are almost the same as those of the starting material within the precision of the method. Similar behaviour of the In-Se amorphous films, obtained under similar deposition conditions, has been reported in [12, 13]. Extraction quantitative structural information about short-range ordering, i.e. the interatomic distances, their standard deviations and the coordination numbers, is the main aim of the present work. It is well known that the interpretation method which correlates the area of the radial distribution function (RDF) peak with the coordination numbers should be regarded only as an approximation because the weighting factors are K dependent [23]. The exact method, proposed by Warren [23] for amorphous samples with more than one atomic species, has been used in this work. Assuming a three-dimensional Gaussian distribution of the interatomic distances with the standard deviation σ (which is the measure of the spread of the interatomic distances), the shape of the one-dimensional radial distribution function $4\pi r^2\rho(r)$ can be expressed by convolution of the Gaussian function, averaged over all orientations, with the peak shape function $P_{ij}(r)$ as follows:

$$4\pi r^2\rho(r) = r\sum_{i=1}^{n}\sum_{j=1}^{n}\sum_{k}\frac{c_i N_{ij}^{(k)}}{\sqrt{2\pi}\sigma_{ij}^{(k)} r_{ij}^{(k)}} \times \int_0^{\infty}\left\{\exp\left[-\frac{\left(r'-r_{ij}^{(k)}\right)^2}{2\left(\sigma_{ij}^{(k)}\right)^2}\right] - \exp\left[-\frac{\left(r'+r_{ij}^{(k)}\right)^2}{2\left(\sigma_{ij}^{(k)}\right)^2}\right]\right\} \times [P_{ij}(r-r') - P_{ij}(r+r')]\,\mathrm{d}r', \quad (1)$$

where

$$P_{ij}(r) = \frac{1}{\pi}\int_0^{K_{\max}}\frac{f_i f_j}{\langle f\rangle^2} W(K)\cos(Kr)\,\mathrm{d}K, \quad (2)$$

ρ_0 is the average atomic density, c_i is the atomic concentration, f_i is the atomic scattering factor, n is the number of the atomic species. The third sum in Equation 1 is taken over all the coordination spheres. $N_{ij}^{(k)}$, $r_{ij}^{(k)}$ and $\sigma_{ij}^{(k)}$ indicate the coordination number, the interatomic distance and its standard deviation of the i-th and j-th kind of atom in the k-th coordination sphere, respectively. In the present work the Lorch window function $W(K) = \sin(\pi K/K_{\max})/\pi K/K_{\max}$ was used for calculations of the RDF. The structural parameters can be extracted from the experimental data using

the curve-fitting method. The computation procedure which utilizes a least-squares routine has been described in detail in [24]. The differences between the calculated and experimental RDF's can be quantified in terms of a discrepancy factor R, defined by the sum of the squares of the residuals, normalized by the sum of the squares of the experimental data points

$$R = \left\{ \frac{\sum_i \left[4\pi r_i^2 \rho_i^{(\mathrm{exp})} - 4\pi r_i^2 \rho_i^{(\mathrm{cal})}\right]^2}{\left[\sum_i 4\pi r_i^2 \rho_i^{(\mathrm{exp})}\right]^2} \right\}^{1/2}. \quad (3)$$

The experimental RDF is related to the corrected and normalized intensity function $I(K)$ as follows:

$$4\pi r^2 \rho(r) = 4\pi r^2 \rho_0 + rG(r), \quad (4)$$

where

$$G(r) = 4\pi r[\rho(r) - \rho_0] = \frac{2}{\pi} \int_0^{K_{\max}} K \frac{I(K) - \langle f^2 \rangle}{\langle f \rangle^2} W(K) \sin(Kr)\, \mathrm{d}K. \quad (5)$$

In Fig. 1 the corrected and normalized to electron units intensity functions are shown together with the independent scattering $\langle f^2 \rangle + I_c(K)$. The Compton intensity $I_c(K)$ was calculated using tabulated values given by Cromer [25] and then multiplied by the recoil factor [26] and the term resulting from increased absorption of the Compton contribution [27]. The values of the atomic scattering factors together with the real and imaginary parts (the anomalous dispersion correction terms) were

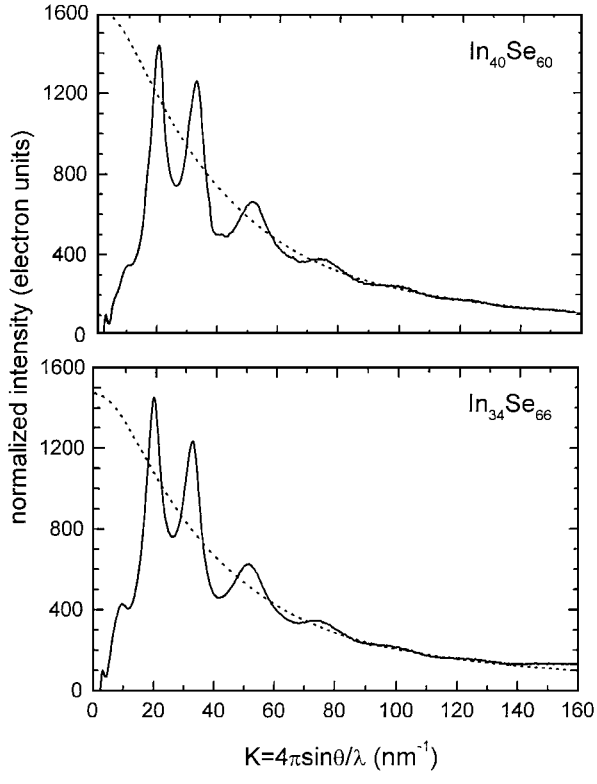

Figure 1 Corrected and normalized X-ray intensities (solid lines) and the independent scattering (dotted line) for $In_{40}Se_{60}$ and $In_{34}Se_{66}$.

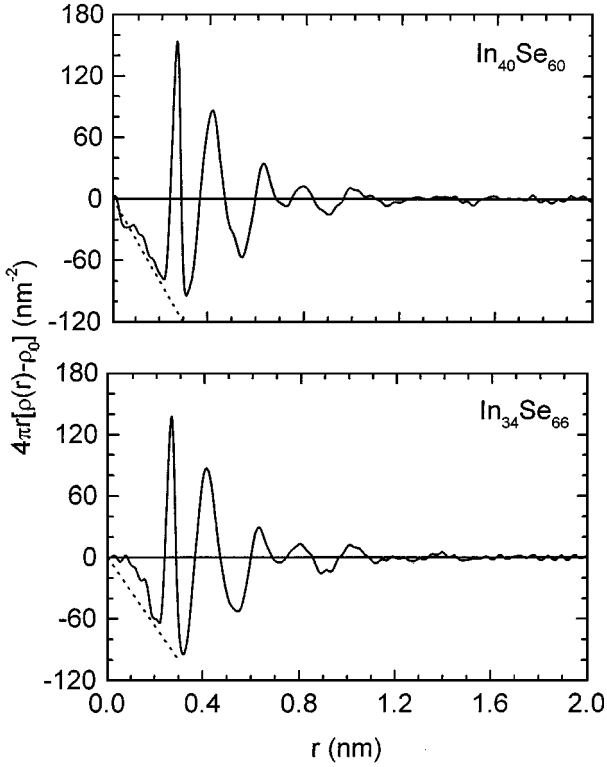

Figure 2 Reduced radial distribution functions $4\pi r[\rho(r) - \rho_0]$ (solid line) for $In_{40}Se_{60}$ and $In_{34}Se_{66}$. $-4\pi r\rho_0$ are plotted as dotted lines.

taken from the International Tables for X-Ray Crystallography [28]. The intensity curves, shown in Fig. 1, oscillate around the independent intensity for both investigated amorphous films. Only little normalization problems were encountered for $In_{34}Se_{66}$ in a high K range. The resulting $G(r)$ functions, shown in Fig. 2, do not contain significant spurious details, which indicate that the correction and normalization procedures were satisfactorily performed. The ρ_0 values of 0.032 and 0.030 for $In_{40}Se_{60}$ and $In_{34}Se_{66}$ were taken for calculations which are less within the 10% limit than the average atomic densities found for the In_2Se_3 and InSe phases [2]. The $-4\pi r\rho_0$ functions are plotted in Fig. 2 as dotted lines. The analysis of the first RDF peaks, performed according to Equation 1, is based on a general assumption that the nearest neighbour coordination number of the corresponding crystal is preserved in almost all amorphous semiconductors [29].

The first attempts to fit the experimental RDF's in the range of 0.23–0.29 nm were made with a one-shell model assuming that only Se is the near neighbour to In. Such a coordination is typical for $A_2^{III}B_3^{VI}$ compounds with the defective zinc blende structure in which 1/3 of the A sites is vacant [30]. The fitting procedures converged to the values listed in Table II. The calculated

TABLE II The one-shell best-fit parameters r, N and σ for the In-Se amorphous films together with the discrepancy factors R

	r (nm)	N	σ (nm)	Atomic pair	R
$In_{40}Se_{60}$	0.262 ± 0.002	3.60 ± 0.25	0.012 ± 0.002	In-Se	0.008
$In_{34}Se_{66}$	0.262 ± 0.002	3.95 ± 0.25	0.013 ± 0.002	In-Se	0.011

TABLE III The multi-shell best-fit parameters (the three-shell fit for $In_{40}Se_{60}$ and the two-shell fit for $In_{34}Se_{66}$) r, N and σ for the In-Se amorphous films together with the discrepancy factors R

	r (nm)	N	σ (nm)	Atomic pair	R
$In_{40}Se_{60}$	0.249 ± 0.005	0.55 ± 0.5	0.014 ± 0.005	Se-Se	0.006
	0.262 ± 0.005	3.00 ± 0.5	0.011 ± 0.005	In-Se	
	0.277 ± 0.005	0.55 ± 0.5	0.014 ± 0.005	In-In	
$In_{34}Se_{66}$	0.252 ± 0.005	0.90 ± 0.5	0.013 ± 0.005	Se-Se	0.012
	0.263 ± 0.005	3.67 ± 0.5	0.013 ± 0.005	In-Se	

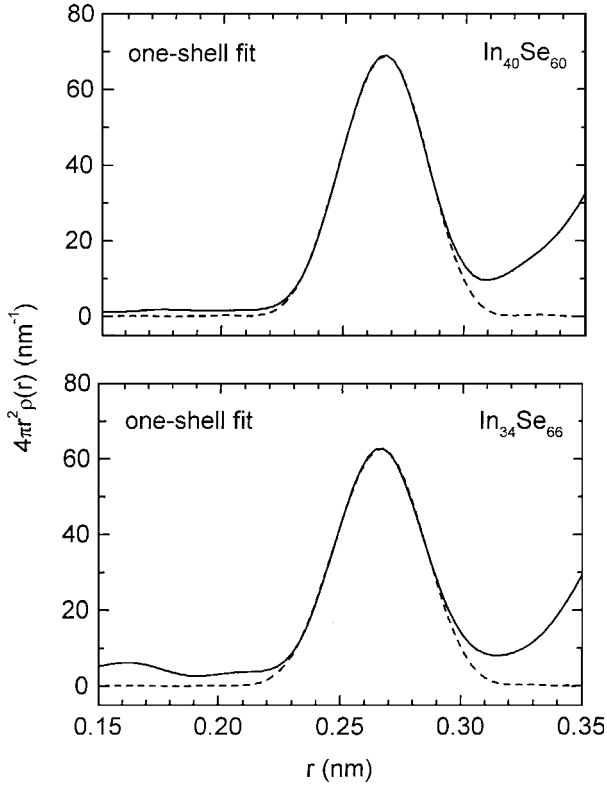

Figure 3 One-shell best-fit model (dashed line) and experimental (solid line) radial distribution functions $4\pi r^2\rho(r)$ for $In_{40}Se_{60}$ and $In_{34}Se_{66}$.

and experimental functions are compared in Fig. 3. Then a series of the model simulations with the distinct In-In, In-Se and Se-Se contributions to the first coordination sphere were carried out. The results of the multi-shell fit are shown in Table III and resulting RDF's are shown in Fig. 4. The obtained results are discussed in the next section.

4. Discussion

A general conclusion can be drawn from comparison of the intensity and radial distribution curves, shown in Figs 1 and 2. In spite of the 6 at.% difference in the chemical composition, the investigated In-Se amorphous films have generally the structure of the same type. However, network sites for $In_{40}Se_{60}$ and $In_{34}Se_{66}$ may be decorated by two atomic species in a different manner, resulting from the film composition. Both the intensity and radial distribution functions have practically the same peak positions and amplitudes. Only in a small K region the prepeak at about 10 nm^{-1} in more

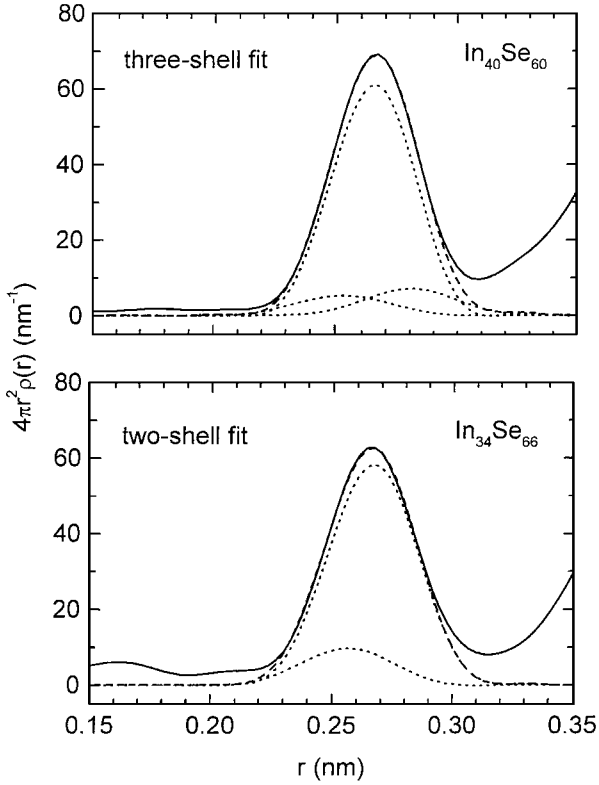

Figure 4 Three-shell ($In_{40}Se_{60}$) and two-shell ($In_{34}Se_{66}$) best-fit model (dashed line) and experimental (solid line) radial distribution functions $4\pi r^2\rho(r)$ for $In_{40}Se_{60}$ and $In_{34}Se_{66}$. The partial contributions are shown as dotted lines.

resolved and intense for $In_{34}Se_{66}$ while in the case of $In_{40}Se_{60}$ a shoulder is observed. The $G(r)$ functions exhibit the well pronounced oscillations up to about 1.1 nm, which indicate that the In-Se films are ordered within this range. Therefore attempts have been made to construct one model describing atomic arrangement for both compositions.

The $N_{\text{In-Se}}$ coordination numbers of 3.6 and 3.95, obtained from one-shell fitting, suggest the tetrahedral coordination of indium for $In_{40}Se_{60}$ and $In_{34}Se_{66}$. The $N_{\text{Se-In}}$ coordination numbers, estimated using the bond-consistency condition:

$$c_{\text{In}} N_{\text{In-Se}} = c_{\text{Se}} N_{\text{Se-In}}, \tag{6}$$

are 2.4 and 2.04 for $In_{40}Se_{60}$ and $In_{34}Se_{66}$, respectively. The near neighbour interatomic distance of 0.262 nm, the same for both samples, is in between the sum of the In_{IV} and Se_{III} covalent atomic radii ($0.144 + 0.120 = 0.264$ nm) and the sum of the In_{IV} and Se_{II} covalent atomic radii ($0.144 + 0.116 = 0.260$ nm), given by Suchet [31]. Assuming that the first coordination sphere is occupied only by atoms of the same kind the tetrahedral coordination of In and the coordination number of Se < 3 can be explained by the model of the defected zinc blende structure with the vacant sites in the indium sublattice (1/3 vacant sites). Such a structure has been found for In_2Te_3 and Ga_2Se_3 [30]. In this model 1/3 of the Se atoms are two-fold coordinated and remaining 2/3 Se are three-fold coordinated which gives the average coordination number of Se 2.67. However, the two-fold coordination of the Se

in $In_{34}Se_{66}$ indicates an increased number of the vacant sites (about 1/2 vacant sites) and a strong distortion of the zinc blende type structure. The tetrahedral coordination of In and the two-fold coordination of Se for $In_{34}Se_{66}$ is inconsistent with this model (In has only three valence electrons). Moreover, in the case of the zinc blende structure, two RDF peaks of a high amplitude are expected at $r = 0.428$ nm (In-In and Se-Se) and $r = 0.502$ nm (In-Se). Instead, only one peak at about 0.41 nm is observed and at about 0.5 nm $G(r)$ exhibits negative peak. From analysis of the RDF's for $In_{40}Se_{60}$ and $In_{34}Se_{66}$ one can conclude that the defective zinc blende model is incompatible with the experimental data and cannot describe satisfactorily the local structure of both films.

In the next stage the model based on the defective wurtzite has been considered. The crystal structure of the low-temperature form of In_2Se_3, determined by Likforman, Carre and Hillel [32], can be regarded as a distorted wurtzite-like structure, in which the In atoms are either tetrahedrally or pentagonally coordinated by Se and the Se atoms have three In as nearest neighbours. In this structure the near-neighbour coordination shell is more complex. The length of In-Se bonds are in the range of 0.252–0.294 nm [32]. The experimental RDF's exhibit a very weak contribution at r of about 0.29–0.30 nm. The $N_{\text{In-Se}}$ coordination number is, on the average, 4.5 and is greater than those found for the In-Se amorphous films. The three fold coordination of Se is also inconsistent with the values 2.4 and 2.04 derived for the $In_{40}Se_{60}$ and $In_{34}Se_{66}$ amorphous films, respectively. Assuming the In_2Se_3 model for $In_{34}Se_{66}$ where the number of the In-Se bonds is maximized and the concentration of In is less than the stoichiometric value 0.40 we have obtained the partial coordinations: $N_{\text{In-Se}} = 4.5$, $N_{\text{Se-In}} = 2.32$, $N_{\text{Se-Se}} = 0.68$, according to Equation 13 in Ref. 33. These estimations are also inconsisted with the experimental data. From this comparison it has been concluded that the structure of the low-temperature form of In_2Se_3 is inappropriate as the model of atomic arrangement in the investigated indium selenide films.

Therefore we analyse the multi-shell models, in which the partial In-In, In-Se and Se-Se contributions are involved in the first coordination sphere. The bonds between atoms of the same kind occur in the indium monoselenide type structure. This structure has been determined by Likforman *et al.* [34] and then refined by Rigoult *et al.* [35]. In the InSe structure the In atoms are coordinated by one In and three Se and each Se has only three In as nearest neighbours. However, the Se content in the investigated amorphous films is greater than 50 at.%. In order to consider the InSe structure as the starting model it has been assumed that the In positions are statistically occupied by In and Se, according to the following formulas: $(In_{0.80}Se_{0.20})Se$ and $(In_{0.68}Se_{0.32})Se$ for $In_{40}Se_{60}$ and $In_{34}Se_{66}$, respectively. Substitution of the In atoms by Se in both films leads to creation of the Se-Se bonds and consequently to the decrease in the coordination numbers $N_{\text{Se-In}}$ and $N_{\text{In-In}}$. The estimated partial coordination numbers, which are consistent with the constraint expressed by Equation 6 and four fold coordination of In and three fold coordination of Se, are: $N_{\text{In-In}} = 0.4$, $N_{\text{In-Se}} = 3.6$, $N_{\text{Se-In}} = 2.4$, $N_{\text{Se-Se}} = 0.6$ for $In_{40}Se_{60}$ and $N_{\text{In-In}} = 0.04$, $N_{\text{In-Se}} = 3.96$, $N_{\text{Se-In}} = 2.04$, $N_{\text{Se-Se}} = 0.96$ for $In_{34}Se_{66}$. The structural parameters obtained from the three-shell fitting procedure for $In_{40}Se_{60}$ are listed in Table III. The three-shell fitting procedure for $In_{34}Se_{66}$, in which all parameters were allowed to vary leads to the $N_{\text{In-In}}$ coordination number of about 0.4, $r_{\text{In-In}} = 0.285$ nm the considerably greater $\sigma_{\text{In-In}}$ value of 0.025 nm which significantly reduces the amplitude of the In-In component. These results suggest that the fitting routine try to eliminate the In-In contribution. Therefore for $In_{34}Se_{66}$ only the In-Se and Se-Se pairs have been assumed to contribute to the first coordination sphere according to the estimated partial coordination numbers ($N_{\text{In-In}} = 0.04$) for the model based on the InSe crystalline structure. The best two-shell fitting parameters are shown in Table III. A comparison of the coordination numbers, expected for the model based on the InSe structure with the experimental findings show that this model explains very well the atomic arrangement in the investigated amorphous films within the first coordination sphere. The interatomic In-Se distances of 0.262 nm and 0.263 nm are the same as those determined in Ref. 34 (0.263 nm). The In-In distances for the amorphous $In_{40}Se_{60}$ film and crystalline InSe are identical (0.277 nm) and less than twice the In tetrahedral radius (0.288 nm). This could be explained by occurrence of In in one of the vertices of Se tetrahedra. Opposite tendency is observed in the case of the Se-Se distances, which is longer than twice the Se_{III} radius (0.244 nm). Such increase could be related to influence of the network when some of In positions are substituted by Se.

Finally we have considered the case of complete chemical disorder for the InSe structure. In the limit of this model the partial coordination numbers are: $N_{\text{In-In}} \simeq 1.88$, $N_{\text{In-Se}} \simeq 2.12$, $N_{\text{Se-In}} \simeq 1.41$, $N_{\text{Se-Se}} \simeq 1.59$ for $In_{40}Se_{60}$ and $N_{\text{In-In}} \simeq 1.63$, $N_{\text{In-Se}} \simeq 2.37$, $N_{\text{Se-In}} \simeq 1.22$, $N_{\text{Se-Se}} \simeq 1.78$ for $In_{34}Se_{66}$, according to Cargill and Spaepen [36]. A comparison of the obtained coordinations and the best-fit parameters presented in Table III clearly shows that the chemically disordered model does not describe satisfactorily the atomic distribution within the first coordination sphere—the estimated In-In and Se-Se coordination numbers are too high in comparison with the experimental values.

The coordination numbers and the near-neighbour distances for the amorphous InSe and In_2Se_3 thin films have been reported by Mot and Davies [37]. These data have been obtained from electron diffraction studies [38, 39], reviewed also by Grigorovici [40]. For a-InSe $N_{\text{In-Se}} = 3.46$, $N_{\text{Se-In}} = 3.46$ and $N_{\text{In-In}} = 0.95$ but with considerably longer $r_{\text{In-In}} = 0.315$ nm have been found. It has been concluded that the short-range configuration present in the InSe crystal is retained in a-InSe. For this comparison the structural data for crystalline InSe with $r_{\text{In-Se}} = 0.250$ nm and $r_{\text{In-In}} = 0.316$ nm has been taken from [41]. The coordination numbers of In and Se, reported in [37], are generally in agreement with the present findings for the $In_{40}Se_{60}$

film. However, the distances between near-neighbours reported by Semiletov [41] differs significantly from those used for interpretation of the X-ray scattering data in the present work and given in [34, 35]. On the other hand the defective zinc blende structure with $N_{\text{In-Se}} = 4$ and $N_{\text{Se-In}} = 2.67$ has been suggested in [37, 39, 40] for the amorphous In_2Se_3 thin films. This conclusion differs from the present suggestions.

In order to discriminate between the one-shell and multi-shell models it is essential to notice that in the present work agreement of the simulations with the experimental data and mutual consistency of the models for both chemical compositions are the criteria of model validity. The one-shell model, based on the defective zinc blende structure may describe satisfactorily atomic arrangement for $In_{40}Se_{60}$ within the first coordination sphere but not in the range of the second RDF peak. In this structure two electrons are transferred from any three Se atoms to two In atoms leading to the formation by each In four sp^3 bonds with the neighbouring Se atoms. Such a bonding scheme, in which both In and Se fill their subshells in the bond formation, cannot be retained for $In_{34}Se_{66}$ where $1/2$ of In sites is vacant and se are two fold coordinated. On the other hand the three-shell model for $In_{40}Se_{60}$ and the two-shell model for $In_{34}Se_{66}$, both based on the InSe type structure, satisfy mentioned above criteria.

5. Conclusions

The wide-angle X-ray scattering technique has been used to characterize short-range ordering in the amorphous $In_{40}Se_{60}$ and $In_{34}Se_{66}$ films. The resulting experimental RDF's, analysed using the curve-fitting method, have provided structural information about structural order, both configurational and chemical. It has been possible to obtain a reasonably good fit to the experimental data using the model based on the InSe structure with the statistically occupied In positions. For the composition at 60 at.% Se three partial components, namely In-In, In-Se and Se-Se contribute to the first coordination sphere. When the Se content is increased the number of the In-In pairs is reduced practically to zero, within the precision of the method. The careful comparison of the experimental and simulated RDF's allowed to test validity of different models and to exclude those of them which are inconsistent with the experimental observations. However, in order to obtain more precise and certain information about the structure of the amorphous In-Se films the further experiments, joint EXAFS and anomalous X-ray scattering seems to be necessary.

Acknowledgement

The authors would like to thank Dr. Denis Raoux for very helpful and valuable discussion.

References

1. J. VAN LANDUYT, G. VAN TENDELOO and S. AMELINCKX, *Phys. Stat. Sol.* (a) **30** (1975) 299.
2. S. POPOVIC, A. TONEJC, B. GRZETA-PLENKOVIC, B. CELUSTKA and R. TROJKO, *J. Appl. Cryst.* **12** (1979) 416.
3. B. DAOUCHI, M. C. RECORD, J. C. TEDENAC and G. VASSILIEV, *Z. Metallkd.* **89** (1998) 612.
4. J. YE, S. SOEDA, Y. NAKAMURA and O. NITTONO, *Jpn. J. Appl. Phys.* **37** (1998) 4264.
5. S. N. SAHU, *Thin Solid Films* **261** (1995) 98.
6. J. F. SANCHEZ-ROYO, A. SEGURA, O. LANG, C. PETTENKOFER, W. JAEGERMANN, A. CHEVY and L. ROA, *ibid.* **307** (1997) 283.
7. M. A. KENAWY, A. F. EL-SHAZLY, M. A. AFIFI, H. A. ZAYED and H. A. EL-ZAHID, *ibid.* **200** (1991) 203.
8. A. J. JACOBSON, *Solid State Ionics* **5** (1981) 65.
9. S. K. BISWAS, S. CHAUDHURI and A. CHOUDHURY, *Phys. Stat. Sol.* (a) **105** (1988) 467.
10. Y. WATANABE, S. KANEKO, H. KAWAZOE and M. YAMANE, *Phys. Rev.* **B40** (1989) 3133.
11. J. C. BERNEDE, S. MARSILLAC, A. CONAN and A. GODOY, *J. Phys.: Condensed Matter* **8** (1996) 3439.
12. S. MARSILLAC, J. C. BERNEDE and A. CONAN, *J. Mater. Sci.* **31** (1996) 581.
13. R. MEHRA, S. KOHLI, A. PUNDIR, V. K. SACHDEV and P. C. MATHUR, *J. Appl. Phys.* **81** (1997) 7842.
14. J. V. MCCANY and R. B. MURRAY, *J. Phys.* **C10** (1977) 1211.
15. K. ANDO and A. KATSUI, *Thin Solid Films* **76** (1981) 141.
16. M. YUDASAKA and K. NAKANISHI, *ibid.* **156** (1988) 145.
17. D. C. JOY, "Monte Carlo simulation in Turbo Pascal" (Glasgow, 1995).
18. J. PHILIBERT and R. TIXIER, *J. Phys.* **D1** (1968) 685.
19. M. ŻELECHOWER, A. DYTKOWICZ, J. CHRAPOŃSKI and I. JENDRZEJEWSKA, in Proceedings of the IX Conference on Electron Microscopy od Solids, Kraków, May 1996, edited by A. Czyrska-Filemowicz (Fotobit, Kraków, 1996) p. 169.
20. D. M. NORTH and C. N. J. WAGNER, *J. Appl. Cryst.* **2** (1969) 149.
21. P. LECANTE, PhD thesis, L'Universite Paul Sabatier de Toulouse (Science), 1990, No. 1417.
22. P. LECANTE, A. MOSSET, J. GALY and A. BURIAN, *J. Mater. Sci.* **27** (1992) 3286.
23. B. E. WARREN, "X-ray diffraction" (Addison-Wesley, Reading MA, 1969) p. 116.
24. A. BURIAN, P. LECANTE, A. MOSSET, J. GALY, J. M. TONNERRE and D. RAOUX, *J. Non-Cryst. Solids* **212** (1997) 23.
25. D. T. CROMER, *J. Chem. Phys.* **50** (1969) 4857.
26. C. W. DWIGGINS and D. A. PARK, *Acta Cryst.* **A27** (1971) 264.
27. F. HAJDU and G. PALINKAS, *J. Appl. Cryst.* **5** (1972) 395.
28. In "International Tables for X-Ray Crystallography, Vol. III" (Kynoch Press, Birmingham, 1969) pp. 71, 149.
29. A. F. IOFFE and A. R. REGEL, *Prog. Semicond.* **4** (1960) 237.
30. F. S. GALASSO, "Structure and properties of inorganic solids" (Pergamon Press, Oxford, 1970) p. 87.
31. J. P. SUCHET, *J. Phys. Chem. Solids* **16** (1960) 265.
32. A. LIKFORMAN, D. CARRE and R. HILLEL, *Acta Cryst.* **B34** (1978) 1.
33. S. J. GURMAN, *J. Non-Cryst. Solids* **139** (1002) 107.
34. A. LIKFORMAN, D. CARRE, J. ETIENNE and B. BACHET, *ibid.* **B31** (1975) 1252.
35. J. RIGOULT, A. RIMSKY and A. KUHN, *ibid.* **B36** (1980) 916.
36. G. S. CARGILL and F. SPAEPEN, *ibid.* **43** (1981) 91.
37. N. F. MOTT and E. A. DAVIS, "Electronic processes in non-crystalline materials" (Clarendon Press, Oxford, 1971) p. 193.
38. L. I. TATARINIVA and T. S. KAZMAZOVSKAYA, *Kristallografiya* **6** (1961) 865.
39. A. I. ANDREYEVSKY, I. D. NABITOVITCH and Y. V. VOLOSHCHUK, *ibid.* **7** (1962) 865.
40. R. GRIGOROVICI, in Proceedings of the 13th Session of the Scottish Universities Summer School in Physics, Electronic and Structural Properties of Amorphous Semiconductors, Aberdeen 1972, edited by P. G. Comber and J. Mort (Academic Press, London, 1973) p. 191.
41. S. A. SEMILETOV, *Kristallografiya* **3** (1958) 288.

Received 28 January
and accepted 23 November 1999